# Determination of the Quadrupole Coupling Constant of the Invisible Aluminum Spins in Zeolite HY with $^1H/^{27}Al$ TRAPDOR NMR

**Clare P. Grey[†] and Alexander J. Vega*[,‡]**

*Contribution from the Department of Chemistry, State University of New York at Stony Brook, Stony Brook, New York 11794-3400, and Contribution No. 7104 from DuPont Central Research and Development, Experimental Station, P.O. Box 80356, Wilmington, Delaware 19880-0356*

*Received March 3, 1995[⊗]*

**Abstract**: The transfer of populations in double resonance (TRAPDOR) NMR method is applied to the $^1H$ and $^{27}Al$ nuclei of Brønsted acid sites in dehydrated zeolite HY. In the experiment, the intensity of a $^1H$ magic angle spinning (MAS) echo signal is reduced by $^{27}Al$ irradiation applied during the evolution period of the echo sequence. A semiquantitative theory is proposed to explain the data. Analysis of the signal reduction as a function of the irradiation-frequency offset allows a determination of the quadrupole coupling constant of the $^{27}Al$ nuclei as well as an estimation of the asymmetry parameter and the geometry of the Al−H vector. This technique provides a means of extracting spin-interaction parameters of quadrupolar nuclei that are otherwise invisible by MAS NMR. The method extends the capabilities of NMR to the characterization of catalytically interesting, but typically invisible, aluminum atoms such as those located at the surfaces of alumina supports and at acid sites.

## Introduction

The characterization of alumina-containing catalytic surfaces by $^{27}Al$ magic angle spinning (MAS) NMR is often hindered by strong electric nuclear quadrupole interactions.[1] Aluminum sites with nearly ideal octahedral or tetrahedral symmetry have relatively weak quadrupole interactions and thus give rise to narrow MAS peaks in well-defined chemical-shift ranges from which the coordination environment can be determined. Penta-coordinated Al can also give narrow NMR peaks in many instances. However, the coordination geometries of structurally interesting aluminum atoms, such as those located at the surfaces of alumina supports or at the acid sites in aluminosilicates, often deviate far from tetrahedral and octahedral symmetry and, hence, are subject to strong quadrupole interactions which broaden their MAS signals beyond detection.[1] Despite the intensive efforts in the area of MAS NMR of zeolites since the early 1980s,[2] the usual NMR characterization of these nuclei is still limited to a mere statement of their "invisibility". Recently, however, several alternative methods have been applied for obtaining more information about the invisible $^{27}Al$ nuclei. For example, Ernst et al.[3] applied an echo pulse sequence to $^{27}Al$ in dehydrated H-zeolites to obtain static central-transition spectra, from which they extracted large quadrupole coupling constants (QCC or $e^2qQ/h$) and asymmetry parameters ($\eta$). They found QCC's as large as 16 MHz, with corresponding central-transition broadenings of more than 100 kHz in a 7-T field.[3] Another approach is the analysis of the effect of the dipolar $^1H/^{27}Al$ interaction on the static line shapes[4] or MAS sidebands[5] of proton spectra of AlOH groups to determine the Al−H distance. In addition,

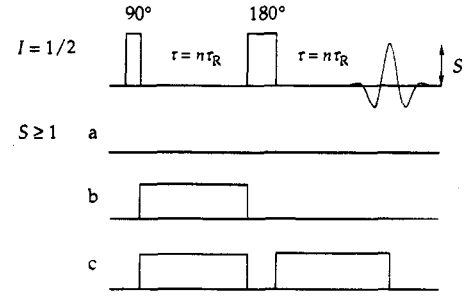


**Figure 1.** The TRAPDOR pulse sequence. A rotor synchronized 90°−180° echo pulse sequence is applied to the $I$ spins while the quadrupolar $S$ spins are irradiated during the evolution period (b), or during both the evolution and the refocusing periods (c). The TRAPDOR fraction is the reduction of the echo signal intensity with respect to that obtained without irradiation (a).

van Eck et al.[6] showed that the existence of a dipolar interaction between an $^{27}Al$ nucleus and a neighboring $I = {}^1/_2$ spin can be detected in a double-resonance experiment, the pulse sequence of which is shown in Figure 1. A rotor-synchronized spin−echo experiment is performed on $I = {}^1/_2$ spins, while irradiation is applied to quadrupolar $S$ spins during the evolution period of the spin−echo. Van Eck et al. used this method to probe the Al/P and Al/Si connectivity in the molecular sieves AlPO-5, NaA, and NaY.[6] Subsequently, Beck et al.[7] and Fyfe et al.[8] applied the method to study $^{27}Al/^1H$ and $^{27}Al/^{29}Si$ couplings, respectively, in zeolites. These results demonstrated that, despite the inability to detect some of the $^{27}Al$ signals directly, it was still possible to manipulate their spin states by the application of an rf pulse. This experiment, which we have named, for

* Author to whom correspondence should be addressed.
† State University of New York at Stony Brook.
‡ DuPont Central Research and Development.
⊗ Abstract published in *Advance ACS Abstracts*, July 15, 1995.

(1) Freude, D.; Haase, J. *Nucl. Magn. Reson. Basic Principles Prog.* **1993**, *29*, 1.
(2) Engelhardt, G; Michel, D. *High-Resolution Solid-State Nuclear Magnetic Resonance of Silicates and Zeolites*; John Wiley & Sons: Chichester, 1987. Fyfe, C. A.; Feng, Y.; Grondey, H.; Kokotailo, G. T.; Gies, H. *Chem. Rev.* **1991**, *91*, 1525.
(3) Ernst, H.; Freude, D.; Wolf, I. *Chem. Phys. Lett.* **1993**, *212*, 588.
(4) Stevenson, R. L. *J. Catal.* **1971**, *21*, 113. Freude, D.; Klinowski, J.; Hamdan, H. *Chem. Phys. Lett.* **1988**, *149*, 355.
(5) Hunger, M.; Freude, D.; Fenzke, D.; Pfeifer, H. *Chem. Phys. Lett.* **1992**, *191*, 391.
(6) van Eck, E. R. H.; Janssen, R.; Maas, W. E. J. R.; Veeman, W. S. *Chem. Phys. Lett.* **1990**, *174*, 428.
(7) Beck, L. W.; White, J. L.; Haw, J. F. *J. Am. Chem. Soc.* **1994**, *116*, 9657.
(8) Fyfe, C. A.; Wong-Moon, K. C.; Huang, Y.; Grondey, H.; Mueller, K. T. *J. Phys. Chem.* **1995**, *99*, 8707.

0002-7863/95/1517-8232$09.00/0 

reasons to become clear shortly, TRAnsfer of Populations in DOuble Resonance (TRAPDOR) NMR,[9,10] is the subject of the present paper. We demonstrate that the application of the TRAPDOR method allows a quantitative determination of large quadrupole coupling constants and an estimation of Al−H distances.

Several research groups, including ours, have been working in recent years on methods of exciting quadrupolar nuclei with very large quadrupole coupling constants. Because of the very broad resonances in polycrystalline samples, it is impossible to excite all the NMR transitions simultaneously with a single pulse. One approach to overcome this problem involves sweeping of the transition frequencies through the resonance condition under cw irradiation, either by varying the frequency of irradiation or by making use of the periodic variations in the quadrupole transition frequencies during MAS experiments. For instance, the method of enhancement of the central transition of $I = {}^5/_2$ nuclei, introduced by Haase et al.,[11,12] involves sweeping the frequency of a continuous irradiation through the satellite transitions of a static sample. An early example of an application of continuous irradiation under MAS conditions is the above-mentioned double-resonance experiment introduced in 1990 by van Eck et al.[6] In 1992, Grey and Veeman reported a $^{13}C/^{14}N/^{1}H$ MAS NMR experiment where an $^{14}N$ irradiation pulse was applied during the evolution period of a $^{13}C$ spin-echo experiment causing a loss of the spin−echo intensities for $^{13}C$ spins in close proximity to the quadrupolar $^{14}N$ nuclei.[13] The proposed explanation of this observation was that the continuous $^{14}N$ irradiation under MAS conditions causes a transfer of populations among the $^{14}N$ Zeeman states. These changes in the spin states of the $^{14}N$ nuclei alter the evolution of the $^{13}C/^{14}N$ coupled spins, so that the $^{13}C$ spins no longer refocus at the rotor echo. The greater the dipolar coupling between the spins, the greater the dephasing and therefore the greater the effect. Recently, the actual occurrence of population transfer between the $^{14}N$ spin states was confirmed by application of a two-dimensional version of the $^{13}C/^{14}N/^{1}H$ experiment.[10]

In a more detailed theoretical explanation of the effect,[14] it was shown that the population transfers occur during avoided level crossings of the quadrupolar spin eigenstates in the rotating frame. These crossings are caused by the time dependence of the quadrupole interaction under magic angle sample rotation. The time dependence is best described in terms of the first-order quadrupole splitting $Q$, which is given by:

$$Q = (\omega_Q/2)[3\cos^2\theta - 1 - \eta\sin^2\theta\cos 2\phi] \qquad (1)$$

where $\eta$ is the asymmetry parameter, $(\theta, \phi)$ are the polar angles that define the orientation of the static magnetic field, $B_0$, with respect to the EFG tensor axes, and $\omega_Q$ is the quadrupole frequency:

$$\omega_Q = 3e^2qQ/[2S(2S-1)\hbar] \qquad (2)$$

Figure 2 shows two examples of the $Q$ dependence of the energy levels (or eigenstates) for a spin $I = {}^5/_2$, under conditions of

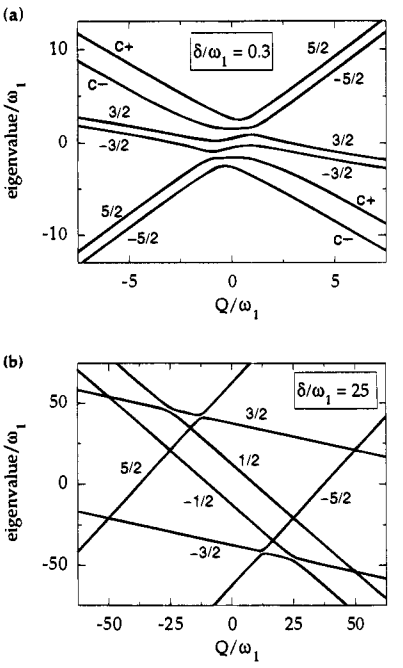


**Figure 2.** Eigenvalues and eigenstates of a spin $^5/_2$ for a rotating-frame Hamiltonian consisting of a quadrupole term ($Q$), a frequency offset term ($\delta$), and an rf term ($\omega_1$). (a) An example of close-to-resonance irradiation: $\delta/\omega_1 = 0.3$. (b) An example of far-off-resonance irradiation: $\delta/\omega_1 = 25$. The eigenstates $m$ are indicated for regions in the plot that are far removed from level crossings. The $c+$ and $c-$ spin states are the sum and difference combinations of $|^1/_2>$ and $|-^1/_2>$ (see Appendix).

continuous rf irradiation. A more detailed description of this quantum-mechanical system is given in the Appendix. Magic angle spinning causes the polar angles $\theta$, $\phi$ to become time dependent, and $Q$ oscillates between large positive and negative values, thus inducing the avoided level crossings seen in the diagrams of Figure 2. As a result, populations are transferred between the different Zeeman levels. This type of population transfer under MAS conditions had been observed earlier in single-resonance spin-locking experiments where the central-transition signal of half-integer quadrupolar nuclei was monitored directly.[15,16] It was also shown that these population transfers have a profound effect on the cross-polarization dynamics of the central transition under conditions of MAS,[17] DOR (double rotation),[18] and DAS (dynamic-angle rotation).[19] These studies pointed out that the population-transfer efficiency of the avoided level crossings depends on the rate of the passages: Adiabatic, i.e., relatively slow, passages through the avoided level crossings result in complete transfer of populations while sudden passages do not induce a transfer. The degree of adiabaticity is determined by the rf amplitude $\nu_1$ applied to the $S$ spins, the sample rotation speed $\nu_R$, and the quadrupole frequency $\nu_Q$. It is quantified by the adiabaticity parameter

$$\alpha' = \nu_1^2/\nu_R\nu_Q \qquad (3)$$

which must be larger than 1 in order to have adiabatic passages.[14−17]

(9) Grey, C. P.; Eijkelenboom, A. P. A. M.; Veeman,W. S.; Vega, A. J., 35th Experimental NMR Conference, Asilomar, 1994.
(10) Grey, C. P.; Eijkelenboom, A. P. A. M.; Veeman, W. S. *Solid State Nucl. Magn. Reson.* **1995**, *4*, 113.
(11) Haase, J.; Conradi, M. S. *Chem. Phys. Lett.* **1993**, *209*, 287.
(12) Haase, J.; Conradi, M. S.; Grey, C. P.; Vega, A. J., *J. Magn. Reson. A* **1994**, *109*, 90.
(13) Grey, C. P.; Veeman, W. S. *Chem. Phys. Lett.* **1992**, *192*, 379.
(14) Grey, C. P.; Veeman, W. S.; Vega, A. J. *J. Chem. Phys.* **1993**, *98*, 7711.
(15) Vega, A. J. *J. Magn. Reson.* **1992**, *96*, 50.
(16) Hayashi, S. *Solid State Nucl. Magn. Reson.* **1994**, *3*, 93.
(17) Vega, A. J. *Solid State Nucl. Magn. Reson.* **1992**, *1*, 17.
(18) Wu, Y.; Lewis, D.; Frye, J. S.; Palmer, A. R.; Wind, R. A. *J. Magn. Reson.* **1992**, *100*, 425.
(19) Fyfe, C. A.; Wong-Moon, K. C.; Grondey, H.; Mueller, K. T. *J. Phys. Chem.* **1994**, 98, 2139. Baltisberger, J. H.; Gann, S. L.; Grandinetti, P. J.; Pines, A. *Mol. Phys.* **1994**, *81* (5), 1109−24.

The principle of the TRAPDOR method is in essence identical to that of the REDOR method.[20] Both experiments interfere with the formation of the rotational echo of a neighboring nucleus $I$ through modification of the heteronuclear dipole interaction during a portion of the echo evolution period and both achieve this by causing changes in the $z$ components of the magnetic moments of the $S$ spins. They differ in that REDOR does it by flipping the $S$ spins with 180° pulses, while TRAPDOR brings it about by adiabatic passages among the Zeeman states. This difference has a fundamental effect on the timing of the spin state changes in the two methods: In REDOR the magnetization changes are simultaneous for all the $S$ spins and take place at times which are externally controlled by the experimenter, whereas in TRAPDOR the spins experience the transfers at times which are largely dictated by the individual orientation dependences of their quadrupolar Hamiltonians, *i.e.*, the spin-state changes are not simultaneous and are controlled by the internal properties of the sample.

In this paper we present TRAPDOR results for $^1H/^{27}Al$ spin pairs in dehydrated zeolite HY where the local environment around the aluminum atoms at the Brønsted acid sites is so distorted that their signal is not visible in the $^{27}Al$ MAS NMR spectrum at our field strength of 7.05 T. The results serve as an illustration of some of the qualitative aspects of the experiment and of the effects of variations in the experimental conditions. A semiquantitative theory for the numerical prediction of TRAPDOR signal reduction is described in the Appendix, along with a critical evaluation of its limitations. The experimental results are compared with those calculated using this theory in the subsection entitled Numerical Results. Results for a high-surface-area form of $AlPO_4$ glass are published elsewhere.[21]

## Experimental Section

Dehydrated H-Y was prepared by deammoniation of $NH_4Y$. The $NH_4Y$ (LZY-62 obtained from Linde) was placed in a sample tube on a vacuum line; the temperature was slowly ramped to 110 °C, held at that temperature for 8 h, slowly ramped to 300 °C, and held at that temperature overnight.[22] The NMR rotors were packed in a glovebag and stored in desiccators until required.

MAS NMR spectra were acquired with a Doty MAS probe using a Bruker CXP-300 spectrometer modified with Tecmag digital and rf circuitry. The $^{27}Al$ Larmor frequency was about 78.2 MHz. The $^1H$ and $^{27}Al$ rf field strengths were adjusted to 50 and 40 kHz, respectively, by monitoring the signal following a single pulse with the length for the desired 180° flip angle of a small ampoule containing an aluminum–nitrate solution. For the TRAPDOR experiments, the sequences shown in Figure 1 were applied with and without $^{27}Al$ irradiation in an alternating fashion, and the two FID's were accumulated separately. This procedure was followed to cancel effects of long-term fluctuations in the spectrometer performance. The TRAPDOR experiment was repeated with varying values of the $^{27}Al$ irradiation frequency (73.7–83.7 MHz in steps of 0.5 MHz) and amplitude (40 or 20 kHz). The experiments were also performed with $^{27}Al$ irradiation during both the evolution and refocusing periods of the echo. Before each run, transmitter and probe were tuned for maximum forward and minimum reflected power as detected with a directional decoupler. Each time, the rf field strength was adjusted to the required level by comparing the amplitude of the forward voltage with the originally calibrated amplitude on the vertical display of an oscilloscope. We made no attempts to evaluate the accuracy of this technique for comparison of rf amplitudes at widely different frequencies, but the symmetry of the TRAPDOR profiles (see below) indicates that the procedure is quite reliable. The recycle delay was 1 s. The typical number of scans was 400 or 800, but in cases of very small TRAPDOR effects it was increased to as much as 8000. Spinning speeds were continuously monitored and found to be stable within ±20 Hz.

A static $^{27}Al$ spectrum of HY was acquired using a Bruker broadbanded probe with a 5-mm coil capable of producing 90° pulses of 3 μs for $^{27}Al$ in an aluminum salt solution. The central-transition spectrum was obtained with a 90°–$\tau$–180° echo sequence using 1- and 2-μs pulses (to account for the effective rf scaling for the central transition of $S = 5/2$ nuclei).[1] $\tau = 20$ μs, 200 ms recycle time, 400 kHz spectral width, and by accumulating 10 000 scans.

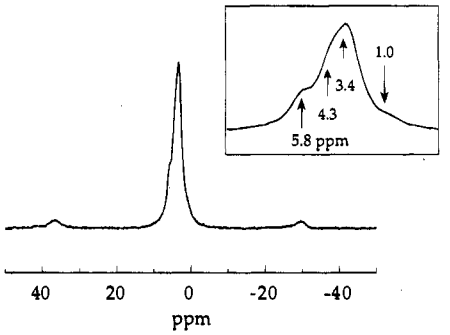


**Figure 3.** The $^1H$ MAS NMR spectrum of deammoniated $NH_4Y$, acquired with a rotor-synchronized spin–echo sequence. A spinning speed of 10 kHz was used and the evolution period of the spin-echo experiment was 100 μs (i.e. one rotor period). The insert shows an expanded view of the centerband.

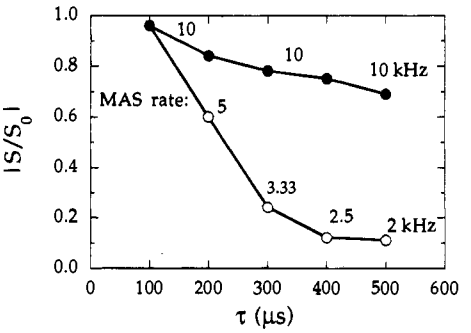


**Figure 4.** Spin–echo signal reduction due to $^{27}Al$ irradiation during the evolution period of a rotor synchronous $^1H$ echo sequence. $|S/S_0|$ is plotted as a function of $\tau$, where $|S|$ and $|S_0|$ are the magnitudes of echo intensities with and without $^{27}Al$ irradiation, respectively. The sample spinning speed is indicated next to the data points. The solid symbols show the change in $|S/S_0|$ for a constant spinning speed of 10 kHz (*i.e.* the number of rotor periods per $\tau$ is varied). The open symbols show the change in $|S/S_0|$ when the spinning speed is changed simultaneously, keeping the rotor period equal to $\tau$. An $^{27}Al$ irradiation frequency of 78.2 MHz and an rf field strength of 40 kHz were used.

## Results

The $^1H$ MAS NMR spin–echo spectrum of deammoniated HY is shown in Figure 3. The main resonance at 3.4 ppm can be assigned to Brønsted acid groups in the supercages of the zeolite, while the shoulder of this resonance (at approximately 4.3 ppm) is due to Brønsted acid groups in the sodalite cages.[23] The resonance at approximately 5.8 ppm represents residual ammonium cations that were not removed during heat treatment of $NH_4Y$, and the weak signal around 1 ppm is due to terminal SiOH groups.

Figure 4 demonstrates the effect of $^{27}Al$ irradiation on the spin–echo intensity of the HY sample when continuous $^{27}Al$ irradiation is applied during the evolution period of the spin–echo sequence (as shown in Figure 1b). On irradiating for only

(20) Gullion, T.; Schaefer, J. *Advances in Magnetic Resonance*; Warren, W. S., Ed.; Academic Press: New York, 1989; Vol. 13, p 57.
(21) Harmer, M. A.; Vega, A. J. *Solid State Nucl. Magn. Reson.* In press.
(22) Luz, Z.; Vega, A. J. *J. Phys. Chem.* **1987**, 91, 374. Kustanovich, I.; Luz, Z.; Vega, S.; Vega, A. J. *J. Phys. Chem.* **1990**, *94*, 3138.
(23) Jacobs, W. P. J. H.; de Haan, J. W.; van de Veen, L. J. M.; van Santen, R. A. *J. Phys. Chem.* **1993**, *97*, 10394.

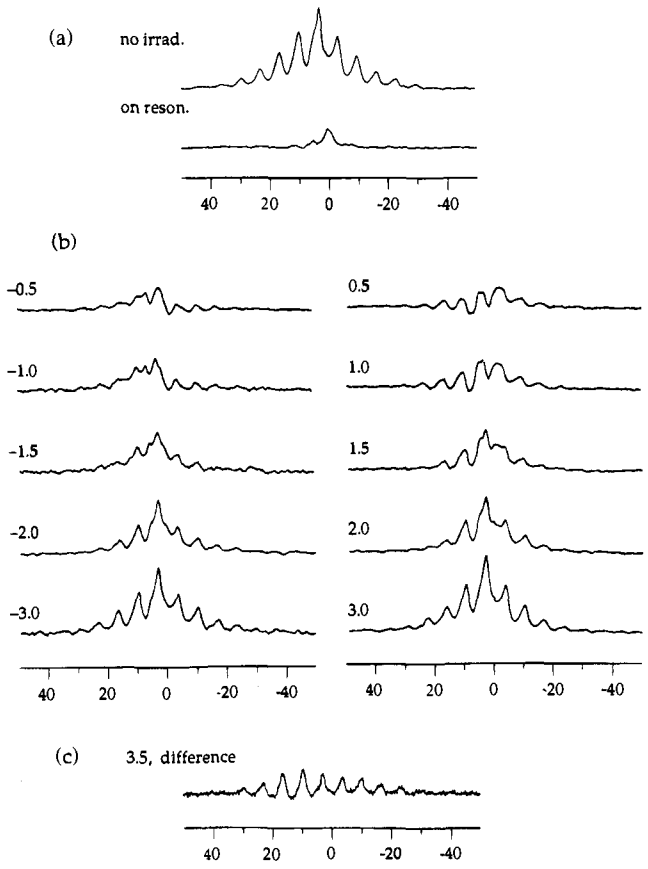


**Figure 5.** The $^1$H echo spectra for a sample of deammoniated $NH_4$–Y, at a spinning speed of 2.0 kHz ($\tau$ = 500 ms) with and without $^{27}$Al irradiation for one $\tau$ period. (a) Comparison of the spectra without and with irradiation at 78.2 MHz, the $^{27}$Al Larmor frequency. (b) Spectra with irradiation at various indicated frequency offsets (in MHz) with respect to 78.2 MHz. (c) The difference between the spectra without and with $^{27}$Al irradiation at a 3.5 MHz frequency offset. The spectra were phase-corrected as described in the text before the difference spectrum was obtained. An $^{27}$Al rf field strength of 40 kHz was used.

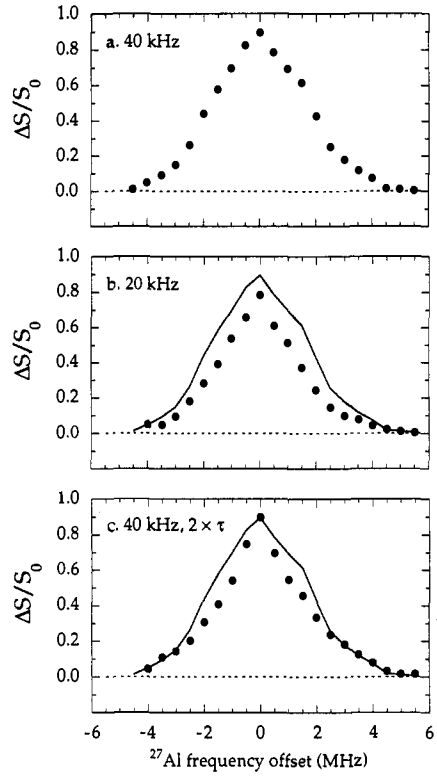


**Figure 6.** The effect of altering the offset of the $^{27}$Al irradiation frequency on the TRAPDOR fraction $\Delta S/S_0$. The frequency offset is measured relative to 78.2 MHz. the $^{27}$Al Larmor frequency. Spinning speed was 2 kHz ($\tau$ = 500 $\mu$s). Irradiation during the evolution period of the $^1$H spin–echo experiment with rf field strengths of (a) 40 and (b) 20 kHz. (c) Irradiation during both the evolution and refocusing periods with an rf field strength of 40 kHz. For comparison, the data in part a are redrawn as a solid line in parts b and c.

100 $\mu$s (*i.e.* one rotor period), only 4% of the signal intensity is lost. Increasing the number of rotor periods of irradiation while keeping the spinning speed constant results in a further gradual decrease in the echo intensity, reflecting an increased accumulation of dipolar dephasing under constant conditions. A much more dramatic effect is observed if the spinning speed is altered while the irradiation time is kept constant. For example, after irradiation for 500 $\mu$s with a spinning speed of 10 kHz (*i.e.*, for five rotor periods), the echo has diminished by 31%, while after irradiation for the same length of time but with a spinning speed of 2 kHz, 89% of the echo intensity has disappeared. This is a manifestation of the impact of the 5-fold increase in the adiabaticity parameter $\alpha'$ when the rotation speed is lowered from 10 to 2 kHz (see eq 3). If the level crossings were completely adiabatic, the accumulated dipolar dephasing would depend on $\tau$ but not on the rotation speed.[14] Hence, the greater echo reduction under slow spinning demonstrates that the efficiency of population transfer decreases with increasing spinning speed, *i.e.*, $\alpha'$ is less than 1 at the highest speed.

The effect of $^{27}$Al irradiation on the proton MAS line shapes is shown in Figure 5 for a rotation speed of 2 kHz and for varying irradiation frequencies. The offset between the applied rf frequency and the Larmor frequency of $^{27}$Al (78.2 MHz) is indicated for each spectrum. The spectra were individually phased in order to obtain flat base lines. (In later sections and the Appendix we discuss the difficulty of achieving satisfactory overall phasing in some of the spectra as well as the actual values of the phase corrections that were employed.) The figures show that the TRAPDOR signal reduction is largest close to the Larmor frequency, but that substantial differences in the echoes can still be observed at offsets of several megahertz. For on-resonance irradiation (Figure 5a), essentially all that remains are the signals of the $NH_4$ and SiOH groups around 6 and 1 ppm, respectively. The sideband manifold in spectra acquired with $^{27}$Al irradiation is not the same as that in the control experiment, and it depends on the $^{27}$Al irradiation frequency. Apparently, the signal reduction is more pronounced in the sidebands than in the centerband. This correlation between sideband intensity and TRAPDOR effect is easily understood, since both are the result of the same heteronuclear dipole interaction. Hence, the crystallites in the powder which, on average, experience the strongest dipolar coupling contribute most to both effects. The effect of irradiation with large-offset irradiation is seen most clearly in the difference spectra (*i.e.*, the control less the $^{27}$Al-irradiation spectrum), for instance as shown in Figure 5c for the offset of 3.5 MHz.

The echo height reduction due to $^{27}$Al irradiation in the evolution period of the spin-echo experiment is plotted against the $^{27}$Al irradiation offset in Figure 6 for the three indicated modes of irradiation. We have chosen to present these data in the form of a "TRAPDOR fraction", defined as the fractional reduction of the absolute intensity of the echo in the time domain,

$$\Delta S/S_0 = (S_0 - |S|)/S_0 \qquad (4)$$

where $S_0$ is assumed to be real by proper choice of the reference phase. To be sure, the phase-sensitive difference of the complex

quadrature signals, $(S_0 - S)/S_0$, reveals more information about the spin system, since TRAPDOR actually affects both the amplitude and the phase of the echo signals,[14] as we already alluded to in connection with Figure 5. However, we avoid using it for several reasons. First, the chosen mode of presentation reduces the quantitation of the effect to a single parameter which is readily measured from the magnitude $|S|$ of the echo signals and allows the TRAPDOR profile to be plotted in a single graph. Second, the determination of $|S|$ is not encumbered by the difficulty of obtaining accurate phase information from experimental spectra like those shown in Figure 5. Third, the phase of $S$ is also affected by a Bloch–Siegert shift (see below),[14,24] which is not related to the dipolar and quadrupolar interactions. The phase shifts are also the main reason why the Fourier transforms of the plain differences of the FID's of $S_0$ and $S$ are difficult to interpret in a straightforward manner, and why the two FID's of $S_0$ and $S$ need to be accumulated in separate files rather than in one file as the difference signal obtained by direct subtraction of the FID's.

The Bloch–Siegert shift is the change in the resonance frequency of spins $I$ (having Larmor frequency $\omega_I$) due to an rf irradiation at frequency $\omega_S$.[24] For $\omega_S \neq \omega_I$ it is given by

$$\delta_{BS} = \omega_I \Omega_I^2/(\omega_I^2 - \omega_S^2) \quad (5)$$

where $\Omega_I$ is the amplitude of one of the rotating components of the rf field as experienced by the $I$ spins. In other words, $\Omega_I$ is given by $\gamma_I B_I$ which in our example is 300/78.2 times larger than the amplitude $\omega_I = \gamma_S B_I$ used elsewhere in this paper. If the irradiation of the $S$ spins is applied during the first $\tau$ period of the echo sequence only, the effect causes a phase shift of $\delta_{BS}\tau$ in the echo signal of $I$, even in the absence of a dipolar interaction. Since $\delta_{BS}$ is the same for all $I$ spins, it does not cause dephasing. For an irradiation amplitude of $\omega_I/2\pi = 40$ kHz at 78 ± 5 MHz the calculated proton shift at 300 MHz is 84 ± 1 Hz. The corresponding Bloch-Siegert phase shift following a 500-$\mu$s pulse is 15°. Experimentally we found that when this experiment was performed with 4 kHz sample rotation ($\tau$ = 250 $\mu$s) on the hydroxyl groups of a non-aluminum-containing high-surface-area silica gel ('Ludox'), the proton echo signals with and without irradiation could be made identical by applying a phase correction of 7°, in agreement with the theoretical prediction. A similar agreement with the predicted phase shift was obtained for TRAPDOR results of HY when the $^{27}$Al irradiation frequency was more than 4 MHz off-resonance. These two control experiments showed in addition that the irradiation did not cause any instrumental artifacts that would influence the phases or amplitudes of the proton signals via mechanisms other than the $^{27}$Al–$^{1}$H dipolar dephasing or the Bloch–Siegert shift.

The population transfers are induced by the rf irradiation whenever the time-dependent resonance frequencies of the quadrupolar satellite transitions pass through the irradiation frequency. In other words, a TRAPDOR effect can only be measured provided the irradiation frequency falls within the boundaries of the first-order quadrupole spectrum. For $S = 5/2$ these come at $\pm 2\nu_Q = (3/10)$ QCC.[1] Hence, the cut-off offsets of ±4.6 MHz in all three TRAPDOR profiles of Figure 6 reveal that the QCC of the anhydrous Brønsted sites in HY is 15.3 MHz.

The TRAPDOR fractions obtained are smaller with an rf strength of $\nu_I$ = 20 kHz than with 40 kHz (Figure 6b). The reason for this difference is that the population transfers are less efficient with weaker rf fields because the adiabaticity parameter scales as $\nu_I^2$ according to eq 3.

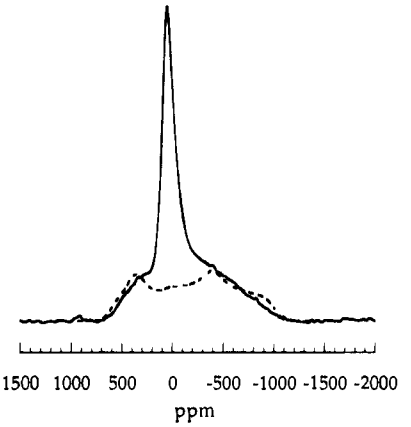


**Figure 7.** A static $^{27}$Al spectrum of deammoniated $NH_4Y$ zeolite obtained with the echo pulse sequence (solid line) and a theoretical central-transition line shape calculated with QCC = 15.3 MHz, $\eta$ = 0.4, a chemical shift of 60 ppm, and a line broadening of 150 ppm (broken line).

Another effect of a variation in the irradiation scheme is demonstrated in Figure 6c. It shows that irradiation of both the evolution and the refocusing periods of the spin-echo sequence gives a smaller TRAPDOR effect than irradiation of one rotor period. This is readily understood if we consider the extreme case of ideal adiabatic passages. Under such conditions, the transfer of populations at every avoided level crossing of the $S$ spin system is complete, ensuring that the population distribution at the end of the rotor cycle returns to what it was at the beginning. The dipolar interactions experienced by the protons during the first $\tau$ period are then exactly repeated during the second period and thus lead to an undisturbed echo. When the passages are not adiabatic, the populations do not return to their original distribution at the end of a cycle and a residual TRAPDOR effect is observed. This is apparently the case under the conditions of Figure 6c.

The static $^{27}$Al echo spectrum of dehydrated HY zeolite is shown in Figure 7. It consists of a broad (overall width ~130 kHz) and a narrow (~30 kHz) component. This spectrum was taken several months after the sample had been prepared. We believe that the narrow component represents Al sites from which the ammonium was not removed by the sample heating and sites that were rehydrated by water that could have been picked up during storage and handling. The narrow peak has about 35% of the total signal intensity. Echo signals measured with $2\tau$ ranging from 40 to 600 $\mu$s gave an exponential decay with $T_2$ = 790 $\mu$s and essentially no $\tau$ dependence of the line shape. The broad component agrees well with the second-order central-transition line shape (broken line) calculated with QCC = 15.3 MHz, $\eta$ = 0.4, a 60 ppm chemical shift, and a 150 ppm Gaussian broadening. This QCC value was derived from the width of the TRAPDOR profile, while the other three parameters were chosen for optimum curve fitting. The parameters do not differ significantly from those recently reported for the quadrupole interaction of $^{27}$Al in dehydrated H–Y: 17.1 ± 1.0 MHz ($\eta$ = 0.6 ± 0.1),[1] 12.7 ± 1.0 MHz ($\eta$ = 0.7 ± 0.1),[3,25] and 13.1 ± 1.0 MHz ($\eta$ = 0.75 ± 0.1)[25] Our chemical shift agrees with the ~60 ppm reported in these publications. The variations in the QCC can be ascribed to differences in sample history and composition.[25] It should be noted that the line shape calculated with one of the published parameter combinations

(24) Bloch, F.; Siegert, A. *Phys. Rev.* **1940**, *57*, 522.

(25) Freude, D.; Ernst, H.; Wolf, I. *Solid State Nucl. Magn. Reson.* **1994**, *3*, 271.

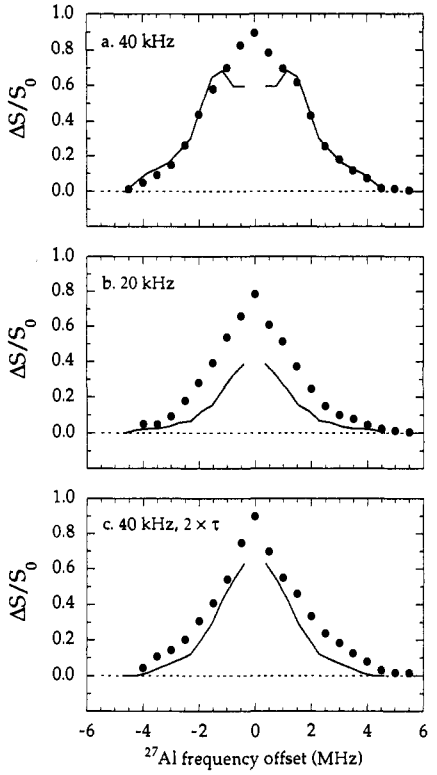


**Figure 8.** Comparison of the calculated (full line) and measured (points) TRAPDOR fractions $\Delta S/S_0$ for deammoniated $NH_4Y$ zeolite due to irradiation during one rotor period with a sample spinning rate of 2 kHz ($\tau$ = 500$\mu$s). (a) Irradiation during the evolution period of the $^1H$ spin–echo experiment with rf field strengths of 40 kHz. (b) Same with 20 kHz. (c) Irradiation during both the evolution and refocusing periods of the spin–echo with an rf field strength of 40 kHz. Numerical parameters for all three plots: $\nu_Q$ = 2.3 MHz (QCC = 15.3 MHz), $\eta$ = 0.4. Al–H distance 2.45 Å. Al–H vector parallel to the $z$ axis of the EFG tensor.

(13.1 MHz, $\eta$ = 0.75) fits the broad part of our experimental spectrum as well as the calculated curve shown in Figure 7, but this QCC must be discarded because it predicts a vanishing TRAPDOR fraction at offsets larger than 3.9 MHz. The actual spectral broadening, which is probably more than the 150 ppm (≈12 kHz) used in the calculation, is larger than the ~2 kHz broadening due to dipolar interaction with the Brønsted proton and is caused by non-uniformity of the structure.

## Numerical Results

The Appendix describes the development of a semiquantitative theory, which allows the TRAPDOR fraction to be calculated under conditions of off-resonance irradiation, for frequency offsets, $\delta$, larger than the rf amplitude. In this section, the experimental and numerical results calculated with this theory are compared. The three experimental TRAPDOR profiles of Figure 6 are plotted in Figure 8, along with the numerical results calculated with the appropriate values of the instrumental parameters and the following internal spin parameters: $\nu_Q$ = 2.3 MHz (QCC = 15.3 MHz), $\eta$ = 0.4, Al–H distance $r$ = 2.45 Å, and the Al–H vector parallel to the $z$ axis of the EFG tensor. These values were chosen as follows. The quadrupole frequency $\nu_Q$ was made equal to one-fourth of the total width of the profile. Since the calculated $\Delta S/S_0$ curve was shown not to be sensitive to ±0.2 variations in the value of $\eta$, whereas the width of the second-order quadrupole broadening has a more pronounced dependence on $\eta$ (provided the QCC is known),[1] we took its value from the curve-fitting result of the central-transition spectrum in Figure 7. The chosen Al–H

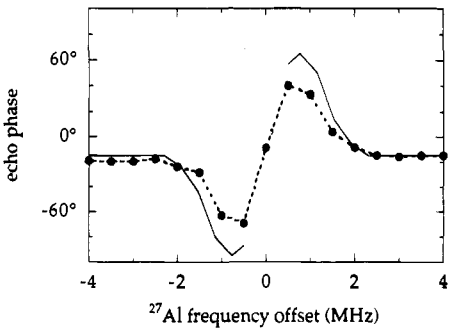


**Figure 9.** Comparison of calculated (line) and measured (connected symbols) phase shift of the TRAPDOR echo $\Delta\varphi = \varphi(S) - \varphi(S_0)$ for deammoniated $NH_4Y$ zeolite, with irradiation during one rotor period. The experimental phases are those required to obtain flat baselines in Figures 4a and 4b. Experimental and numerical parameters are identical to those in Figure 10a. The calculated phase is due to the combined TRAPDOR and Bloch–Siegert effects.

distance represents an average of the distances obtained by NMR for Brønsted acid sites in dehydrated H-zeolites.[4,5,26] Finally, the polar angles for the direction of the internuclear vector with respect to the EFG tensor were adjusted for optimum agreement with the data for 40 kHz irradiation during one $\tau$ period (Figure 8a). The quality of the resulting fit between the experimental and calculated TRAPDOR data is remarkable. Unfortunately, for the lower rf field strength of 20 kHz (Figure 8b) and for irradiation in both $\tau$ periods (Figure 8c) the fits are not so good. In both these cases the calculated TRAPDOR fractions are indeed smaller than in Figure 8a, as was qualitatively predicted in the Results Section, but the large quantitative theoretical differences are not vindicated by the experiment. However, similar values for the magnitude of the quadrupole coupling constant are predicted, and the theoretical curve still maps out a similar overall profile of $\Delta S/S_0$ as a function of the $^{27}Al$ irradiation frequency.

As mentioned above in connection with Figure 5, the proton echo spectra obtained with $^{27}Al$ irradiation do not have the same phase as the ones obtained without. This is partly due to the Bloch–Siegert shift, but the phases are also shifted by the TRAPDOR effect itself (see Appendix). An estimate of the experimental phase shifts is provided by the phase corrections needed to obtain flat baselines in the spectra of Figure 5. These phase corrections (measured with 40 kHz irradiation during the evolution period) are plotted in Figure 9 together with the phases of the calculated FID signals at the top of the echoes. The agreement is quite good. The discrepancy is partly the result of contributions from the non-AlOH proton signals, which are not affected by the TRAPDOR but add a relatively large intensity contribution to the TRAPDOR-reduced signals when the irradiation is close to resonance.

## Discussion

We have applied both methods of static $^{27}Al$ echo spectra and offset-dependent TRAPDOR measurements to obtain an estimate of the quadrupole coupling parameters of the Brønsted Al sites in dehydrated zeolite HY. We found that TRAPDOR provided the most reliable value for the QCC in a straightforward manner. Once its value was known, the asymmetry parameter was most accurately determined by analysis of the echo line shape. However, since the width of the broad portion of the second-order line shape scales as the square of QCC and roughly as $(1 + \eta)$,[1] it is difficult to estimate these two

(26) Kenaston, N. P.; Bell, A. T.; Reimer, J. A. *J. Phys. Chem.* **1994**, *98*, 894.

parameters simultaneously from the central-transition line shape alone: the line shape in Figure 6 could be fitted with the combination 15.3 MHz/0.4, for QCC/$\eta$, as well as with 13.1 MHz/0.75. Another disadvantage of the spin–echo method is that the range of the quadrupole spectrum which can be detected with $^{27}$Al pulses is limited by the ability to excite the total line shape. This limitation can be overcome by stepping the excitation frequency and mapping the height of the echo as a function of the frequency. In fact, we have taken the spectrum shown in Figure 7 at various frequencies to verify that the edges were detected without distortion. Care should also be taken to ensure that the spectral width is sufficient to accommodate the entire spectrum. TRAPDOR is likely to be the preferred method for characterization of Al atoms when there are distinct individual surface sites, provided these sites are coupled to $I = {}^1/_2$ spins having different chemical shifts. In such a situation the central-transition spectrum will consist of overlapping components which are very difficult to deconvolute. Obviously, TRAPDOR can only be used to probe sites that are in close proximity to other spins that are easily detected with a rotor-synchronized echo sequence. Conversely, however, TRAPDOR can be used to help assign resonances of spins that are in proximity to the quadrupolar nucleus.[6-8]

One of the most important limitations to the applicability of $^1$H TRAPDOR is the $T_2$ relaxation time of the proton echoes, since it determines the longest pulse spacing $\tau$ and the lowest spinning speed that can be employed. Longer $\tau$ periods increase the dipolar dephasing and lower spinning speeds improve the population transfers of the quadrupolar spins. Therefore, the TRAPDOR effect is optimized by adjusting the rotor period $\tau_R$ to the longest practical value of $\tau$. The experiment is less effective if the spinning speed is increased to match $\tau = n\tau_R$ with $n \geq 2$. Furthermore, the method works best when the irradiation is applied to only one of the two $\tau$ periods.

The semiquantitative theory is successful in predicting the observed TRAPDOR fractions under at least one set of experimental conditions, *i.e.*, with a sample spinning speed of 2 kHz and an rf irradiation of amplitude $\nu_1 = 40$ kHz during one $\tau$ period (Figure 8a). Calculation of the double-period irradiation did not give equally good agreement (Figure 8c), but the deviation was not very large and may be due to an accumulation of errors. The disagreement between theory and experiment is more severe in the case of the low-amplitude rf irradiation of $\nu_1 = 20$ kHz (Figure 8b). The passages between Zeeman levels in this case are much faster than adiabatic. A value for $\alpha' = 0.09$ can be obtained from eq 3 for the adiabaticity parameter of the powder. In contrast, $\alpha' = 0.35$ when the amplitude is 40 kHz. The semiquantitative method appears to be less successful at predicting the TRAPDOR fraction when the passages are nonadiabatic. In this regime the creation of non-spin locked components becomes important (see Appendix). In the present TRAPDOR case with 20 kHz irradiation, the actual passages appear to be more adiabatic than predicted. In fact, the experimental profile in Figure 8b can be fitted with a calculated curve, provided the numerical value of $\nu_1$ is set to 30 kHz, corresponding to $\alpha' = 0.20$. Even under these non-adiabatic conditions, however, a similar value of the magnitude of the quadrupole coupling constant is still predicted, and the theoretical curve does map out the same overall profile of $\Delta S/S_0$ as a function of the $^{27}$Al irradiation frequency. Thus the theory does allow an estimate for the QCC to be made, even in cases where the experimental values of $\Delta S/S_0$ are not predicted accurately.

The strongest TRAPDOR effects are observed when the irradiation is applied close to the Larmor frequency of the quadrupolar spins. This makes it possible to observe the echo signal reduction and to apply it for establishing atomic connectivities without having to search for the optimum offset frequency. Unfortunately, the current theory is invalid on resonance and does not provide a quantitative interpretation of the TRAPDOR fraction under these preferred conditions. Further calculations and experiments are required to explore the case of on-resonance irradiation more fully.

## Conclusions

We have demonstrated that the $^1$H/$^{27}$Al TRAPDOR technique allows the determination of the quadrupole coupling tensors of $^{27}$Al nuclei which, until recently, were considered to be unobservable by NMR. The quadrupole coupling constant of $^{27}$Al nuclei coupled to protons is obtained with high accuracy, while other quantities such as the asymmetry parameter and the $^1$H–$^{27}$Al distance can also be determined, albeit with less certainty. The TRAPDOR method was compared to the recently introduced static spin–echo method. Since the TRAPDOR effect on the $^{27}$Al spins is observed via the $^1$H spins, $^1$H/$^{27}$Al TRAPDOR can exploit the high resolution of the proton MAS spectra, enabling the characterization of specific sites in complex materials. In particular, the method promises to provide information on aluminum atoms located at the chemically most interesting, but spectroscopically least accessible sites of catalysts and high-surface materials. The intensity of the $^1$H resonance of the Brønsted acid hydroxyl group was selectively reduced by the $^1$H/$^{27}$Al TRAPDOR experiment: only the $NH_4$ and SiOH resonances remain for on-resonance $^{27}$Al irradiation. We presented a theory which describes the effects observed in the $^1$H/$^{27}$Al TRAPDOR experiment under adiabatic and near-adiabatic conditions. Despite some inadequacies of the semi-quantitative approach, the numeric predictions were in quite good agreement with experimental results. The limitations of the theory were addressed at length. The method has been applied to detect the invisible $^{27}$Al spins in anhydrous zeolite HY and to obtain a value of the quadrupole coupling constant of these spins of 15.3 MHz and an asymmetry parameter of 0.4.

**Acknowledgment**. R. O. Balback is thanked for help in preparing the samples and in acquiring the NMR data. Insightful comments of Professor S. Vega are gratefully acknowledged. Acknowledgment is made to the donors of the Petroleum Research Fund, administered by the American Chemical Society, and the NSF National Young Investigator program (DMR 9458017) for partial support of this research.

## Appendix: Theory

In an earlier publication[14] we presented a theoretical model for the prediction of echo-intensity reduction in a TRAPDOR experiment applied to an $I = {}^1/_2$, $S = 1$ spin pair. Detailed calculations were performed for close-to-resonance irradiation of $S$ and for perfectly adiabatic population transfer. In other words, the frequency offset $\delta$ of the irradiation frequency relative to the Larmor frequency of the $S$ spins was assumed to be smaller than the rf amplitude $\omega_1$, and the sample rotation was assumed to be slow. The adiabatic transitions among the $S = 1$ spin states were described as transformations between the Zeeman-order state and the quadrupole-order state, which were represented by density-matrix operators $S_z$ and $Q_z$, respectively. Extensions to off-resonance radiation and slightly nonadiabatic passages were indicated but not worked out in detail. Presently, we propose a semiquantitative model for predictions of TRAPDOR signals with much wider applicability. First, the $I = {}^1/_2$

spins are coupled to quadrupolar nuclei with any spin $S \geq 1$. Second, we drop the requirement of adiabatic (*i.e.* relatively slow) sample rotation and, third, we allow for irradiation off resonance. However, the model does require that frequency offsets must be larger than the rf amplitude ($\delta \gg \omega_1$), thus excluding irradiation on or close to resonance. One may appreciate the need for this limitation by inspection of Figure 2 which shows eigenvalue diagrams for irradiation close to resonance (a) and far off resonance (b) for a quadrupolar spin $S = {}^5/_2$. The diagrams are plots of the eigenvalues of a rotating-frame Hamiltonian consisting of a quadrupole term, a frequency-offset term, and an rf term,

$$H_S = (Q/2)[S_z^2 - S(S+1)/3] + \delta S_z + \omega_1 S_x \qquad (6)$$

$Q$ is the first-order splitting of the quadrupole spectrum defined in (2). Because of the particular form of the time dependence of $\theta$ and $\phi$ during a MAS experiment, the quadrupole splitting $Q$ of every crystallite in a polycrystalline sample oscillates and passes through zero two or four times per rotor cycle. This results in periodic passages through the avoided level crossings shown in Figure 2 and gives rise to the desired transfer of population among the spin states of $S$.

The two diagrams in Figure 2 differ in the complexity of their crossing patterns: in the $\delta < \omega_1$ case (a) all six levels are simultaneously involved in the level crossing, while the level crossings occur separately in pairs when $\delta \gg \omega_1$ (b). Theoretically, very slow sample-rotation conditions will render every passage adiabatic and ensure total population transfer among connected eigenstates. For instance, under close-to-resonance irradiation the populations of the $\pm{}^5/_2$ levels are transferred adiabatically to the $c\pm$ states and vice versa. ($c+$ and $c-$ are the sum and difference combinations of $+{}^1/_2$ and $-{}^1/_2$.)[15,17] Since the population difference between $c+$ and $c-$ is observable as a central-transition NMR signal,[15] the passages should then be detectable as the disappearance and reappearance of the central-transition signal in a spin-lock experiment applied to $S = {}^5/_2$ spins. This effect was indeed observed for $S = {}^3/_2$ nuclei when the adiabaticity parameter $\alpha' = \omega_1^2/\omega_Q\omega_R$ was not significantly smaller than 1.[15,16] However, the results of several MAS spin-lock experiments performed by us on central-transition $^{27}$Al signals have shown that the population transfer is far from complete even for $\alpha' > 3$.[27] This indicates that truly adiabatic conditions for spins ${}^5/_2$ are very difficult to achieve in practice. We believe that we have a rather reliable procedure for predicting the population transfer between just two anti-crossing energy levels (see below), but a good theory for the effective description of multiple anti-crossings is presently out of reach. For a complete prediction of such a nonadiabatic population transfer one would need to provide a $6 \times 6$ matrix simulating the transformation of the population vector induced by the crossing. That matrix would depend on the rate of the passage, the rf intensity, and the frequency offset. An additional complication would be that on-resonance irradiation also affects the $c\pm$ states outside the region of the level crossing, imposing a nutation frequency on some relevant portions of the quadrupolar spin state and modifying the manner in which a neighboring $I$ spin evolves under the dipolar interaction. We currently lack the tools to develop an easily applicable method to predict the TRAPDOR signal intensities when $\delta \leq \omega_1$.

In contrast, off-resonance population transfer in a quadrupolar $S = {}^5/_2$ spin system appears to be understood quantitatively, as was recently demonstrated in $^{27}$Al experiments on a single crystal where the level crossings were induced by sweeping the

(27) Vega, A. J. Unpublished results, 1994.

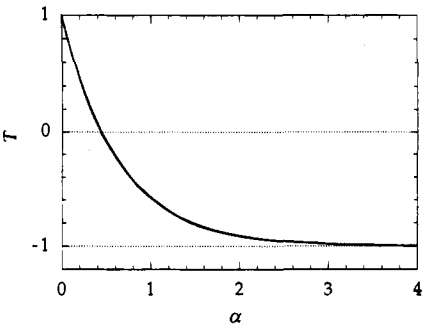


**Figure 10.** The population-transfer function $T$ for the passage of a single avoided level crossing, plotted as a function of the adiabaticity parameter $\alpha$. The function may be parametrized as: $T(\alpha) = 1 - \pi\alpha + 2.329\alpha^2 - 0.754\alpha^3$ for $\alpha < 0.8$; $T(\alpha) = -0.947 - 0.541/\alpha + 1.516/\alpha^2 - 0.609/\alpha^3$ for $0.8 < \alpha < 5$; $T(\alpha) = -1.000$ for $\alpha > 5$. $T(\alpha)$ vanishes for $\alpha \approx 0.44$.

irradiation frequency.[12] For any pairwise level crossing, the extent of population transfer was shown to be a function of a single adiabaticity parameter, determined by the rate of change of the level splitting $d\Delta(t)/dt$ (in the absence of rf irradiation) and by the minimum energy difference $\Delta_{min}$ at the crossing (in the presence of the rf field). Here, we define the adiabaticity parameter as:

$$\alpha = \Delta_{min}^2/|d\delta/dt| \qquad (7)$$

Note that this definition of $\alpha$ refers to a single level crossing, in contrast to that of $\alpha'$ defined in eq 3, which is an estimated average for the entire rotating powder. A universal plot quantifying the amount of population transfer as a function of $\alpha$ is shown in Figure 10. It is derived from a numerical integration[12] of the Bloch equations (without relaxation terms) for a situation where the magnetization, which originally points along the $z$ axis, is subjected to an rf field and a passage of the Zeeman field from far above to far below resonance ($\delta = 200\omega_1 \rightarrow -200\omega_1$). In this case, $\alpha = \omega_1^2/|d\delta/dt|$. At the end of a passage, the normalized $z$ magnetization is 1 if the passage was sudden ($\alpha \ll 1$) and $-1$ if it was adiabatic ($\alpha \gg 1$). The calculated post-passage $z$ magnetization is plotted as the transfer function $T(\alpha)$. In terms of the density matrix of the two-level system for a spin ${}^1/_2$ nucleus, $T$ is the difference between the two diagonal elements following the passage (*e.g.*, the diagonal elements are ${}^1/_2$ and $-{}^1/_2$ when $T = 1$; 0 and 0 when $T = 0$; $-{}^1/_2$ and ${}^1/_2$ when $T = -1$). When applying this to an isolated level crossing in a multilevel system, we use $T$ as the factor which multiplies the population difference before the crossing to yield its value after the crossing. The sum of the level populations is kept constant. In practice, the function is applied in the parametrized polynomial form given in the caption of Figure 10. (The coefficient $-\pi$ of the linear term for small $\alpha$ was determined from an average-Hamiltonian calculation performed in the rotating frame, where the rf field is constant.)[12]

The magnetization will have a sizable $x$, $y$ component, following passages with $\alpha$ between 0.1 and 2, which is represented in the density matrix by rapidly oscillating off-diagonal elements. However, in the present TRAPDOR model such off-diagonal density-matrix elements will be ignored entirely (see below).

For the application of the universal $T(\alpha)$ function to off-resonance level crossings of a quadrupolar spin ${}^5/_2$, we need to evaluate the $Q$ values for which the crossings occur (see Figure 2b) as well as $d\Delta/dt$ and $\Delta_{min}$ for every possible crossing. The $Q$ values at the crossings and the level-crossing rates can be obtained from the expressions for the eigenvalues $E_m$ of $H_S$ in

the absence of rf irradiation:

$$E_{\pm 1/2} = -4Q/3 \pm \delta/2$$

$$E_{\pm 3/2} = -Q/3 \pm 3\delta/2$$

$$E_{\pm 5/2} = 5Q/3 \pm 5\delta/2 \quad (8)$$

There are four single-quantum crossings: $\pm^1/_2 \leftrightarrow \pm^3/_2$ at $Q = \mp\delta$ with $|d\Delta/dt| = |dQ/dt|$, and $\pm^3/_2 \leftrightarrow \pm^5/_2$ at $Q = \mp\delta/2$ with $|d\Delta/dt| = 2|dQ/dt|$. They occur when a transition frequency of an inner or an outer satellite passes by the irradiation frequency. The corresponding minimum level splittings at the crossings are determined by the matrix elements of the rf Hamiltonian.[12] They are $\Delta_{min} = 2\omega_1\sqrt{2}$ for $\pm^1/_2 \leftrightarrow \pm^3/_2$, and $\Delta_{min} = \omega_1\sqrt{5}$ for $\pm^3/_2 \leftrightarrow \pm^5/_2$. This leads to the adiabaticity parameters $\alpha(\pm^1/_2 \leftrightarrow \pm^3/_2) = 8\omega_1^2/|dQ/dt|$ and $\alpha(\pm^3/_2 \leftrightarrow \pm^5/_2) = (^5/_2)\omega_1^2/|dQ/dt|$.

Figure 2b shows that, in addition to the four single-quantum crossings, there are eight multiple-quantum level crossings. For example, the $\Delta m = 2$ crossing of $m = -^1/_2$ with $m = -^5/_2$ occurs when $Q = 2\delta/3$. Although the residual splitting is not resolved in the plot of Figure 2b, the level crossing is avoided by a second-order rf effect given by $\Delta_{min} = 2\omega_1^2\sqrt{10}/Q$ (see Table 1 in ref 12). The rate of passage for this level crossing is $|d\Delta/dt| = 3|dQ/dt|$. Hence, the adiabaticity parameter is $\alpha = 30\omega_1^4/|\delta^2 dQ/dt|$. Similarly, for the $\Delta m = 2$ crossing of $m = ^1/_2$ with $m = -^3/_2$, which occurs when $Q = 2\delta$, we calculate $\alpha = 18\omega_1^4/|\delta^2 dQ/dt|$. In frequency-swept experiments the population-transfer effects of $\Delta m = 2$ level crossings were indeed observed to follow the behavior predicted for the theoretical $\alpha$ values.[12] However, by approximating $|dQ/dt|$ as $\omega_Q\omega_R$, we find that, with typical experimental values ($\nu_1 \leq 40$ kHz, $\nu_Q \geq 1$ MHz, $\nu_R \geq 2$ kHz), the double-quantum $\alpha$ values are <0.15 at an offset of 0.5 MHz, <0.04 at an offset of 1 MHz, etc. Hence, double-quantum level crossings behave mostly as sudden passages having no effect on the level populations. An appreciable degree of double-quantum population transfer will only be encountered when the irradiation frequency differs <1 MHz from the Larmor frequency. Multiple-quantum level crossings of third and fourth order have negligibly small adiabaticity parameters under all considered circumstances.

We now turn to the effect of the dipolar interaction $\omega_D I_z S_z$ on the NMR signal of $I$ following a 90° pulse applied to $I$. In the case of $S = ^1/_2$, the evolution of the density matrix due to this interaction is often described as a linear combination of $I_x$ and the product operator $I_y S_z$. This formalism is particularly convenient for the analysis of REDOR signals because the application of a 180° pulse to the $S$ spins is readily implemented as a change of sign of the $I_y S_z$ term.[20] For the theory of TRAPDOR effects involving $S = 1$, a similar approach also proved useful.[14] Here, the theory had to deal with the modulation of the $S_z$ state caused by the population transfers. However, these changes of level populations could not be characterized by a mere change in the coefficient of $S_z$, because the population changes were of a more general character. It was therefore necessary to invoke a second diagonal spin operator, $Q_z$, to fully describe the $S$ part of the product operators.[14] Applying a similar approach to treat the population transfers for the case of $S = ^5/_2$ would necessitate the use of five independent diagonal spin operators. As long as we may ignore off-diagonal elements of the density matrix of $S$, these five operators form a sufficient set. However, they require an elaborate set of rules for the evaluation of their products which come up in the product-operator calculations. In addition, the description of population transfer between two levels requires the development of a cumbersome algebra in that operator space.

It is more convenient to work with the following alternative formalism, which is equivalent to the product-operator description, provided there are no off-diagonal elements in the density matrix of $S$. We begin with considering a situation where the $I$ spins belong to crystallites with identical orientation (a "single crystal"). Immediately following the 90° pulse the $I$ spins point along, say, the $x$ direction in the transverse plane of the rotating frame of $I$. This collection of spins can be divided into six groups corresponding to the magnetic quantum number $m$ of the neighboring $S = ^5/_2$ spin: $m = ^5/_2, ^3/_2, ..., -^5/_2$. If no pulses are applied to the $S$ spins and no population transfer occurs, the quantum numbers $m$ remain equal to the original value $m_0$ they have at $t = 0$. The $x$, $y$ phase $\varphi(m_0)$ of $I$ spins which are associated with $S$ spins in state $m_0$ will increment in time according to the differential equation:

$$(d/dt)\varphi(m_0) = m_0\omega_D(t) \quad (9)$$

Here, $\omega_D(t)$ is the time-dependent dipolar interaction,

$$\omega_D(t) = (\hbar\gamma_I\gamma_S/r^3)[3\cos^2\beta(t) - 1] \quad (10)$$

where the parameters have the usual meaning. The total FID is then given by:

$$f(t) = (1/6)\sum_{m_0} \exp[i\varphi(m_0)] \quad (11)$$

Under MAS conditions the time dependence of $\beta(t)$ is such that the accumulated phase at the end of a rotor period vanishes. Hence, $f(\tau_R) = 1$. This result is obtained for any crystallite, leading to full echo formation in a polycrystalline sample. In the presence of off-resonance irradiation of $S$, there will be single-quantum and double-quantum population transfers which change the constitution of the magnetic quantum numbers of $S$ spins associated with the $I$ spins labeled $m_0$. To describe this new situation we assign a population vector $p(m_0,m)$ specifying the population distribution over $m$ for $S$ spins that were originally in the $m_0$ state. Thus, at time $t = 0$, $p(m_0,m) = 1$ for $m = m_0$ and 0 for $m \neq m_0$. A level crossing of $m$ with $m'$ induces a transfer of population, which according to the model presented above can be evaluated from the sum and difference populations before the crossing:

$$p_{sum} = p(m_0,m) + p(m_0,m')$$

$$p_{diff} = p(m_0,m) - p(m_0,m') \quad (12)$$

and from the adiabaticity parameter $\alpha$, to produce

$$p(m_0,m) = (1/2)p_{sum} + (1/2)T(\alpha)p_{diff}$$

$$p(m_0,m') = (1/2)p_{sum} - (1/2)T(\alpha)p_{diff} \quad (13)$$

after the crossing. The subsequent phase accumulation of spins $I$ that were originally associated with $S$ spins in state $m_0$ is found by integration of:

$$(d/dt)\varphi(m_0) = \sum_m p(m_0,m)m\omega_D(t) \quad (14)$$

The echo signal, *i.e.*, the sum of the six FID's at $t = \tau_R$, is now <1, the reduction representing the TRAPDOR effect.

In the numerical calculations, the echo signals are integrated over the three Euler angles of the crystallite orientations at time $t = 0$. For each crystallite, the EFG and the internuclear vector

are rotated in small time increments about the magic angle axis. $Q$ and $\omega_D$ are evaluated for each step, the phases of the FID are incremented according to (14), and whenever a level crossing is encountered, the six $p(m_0,m)$ vectors are adjusted according to the appropriate $\alpha$ value derived from the numerically calculated derivative $dQ/dt$. This gives the total echo signal $S$ at the end of the first rotor cycle. The total signal calculated without population transfer is $S_0$.

In general, $S$ does not have the same phase as $S_0$, as was demonstrated previously for $S = 1$.[14] This can be understood by comparing the histories of, for instance, $S$ nuclei beginning in state $m_0 = {}^3/_2$, to those of spins beginning in $m_0 = -{}^3/_2$, for the case of a rotor cycle with $Q$ changing from a large positive to a negative and back to a positive value. Adiabatic single-quantum passages convert $m = -{}^3/_2$ to $-{}^1/_2$ and back to $-{}^3/_2$, while they convert ${}^3/_2$ back and forth to ${}^5/_2$ (see Figure 2b). Hence, the accumulated phases $\varphi(m_0)$ of $I$ will not satisfy the antisymmetry relation $\varphi({}^3/_2) = -\varphi(-{}^3/_2)$, and the out-of-phase contributions to the signals of $m_0 = {}^3/_2$ and $-{}^3/_2$ will not cancel each other at the time of the echo. A similar phenomenon does not exist in REDOR experiments, because there the 180° pulses affect the $m$ and $-m$ states equally and simultaneously.

There is no reason to expect that the phases of the echoes of all individual spin packets will be shifted equally. The spinning sideband manifolds shown in Figure 5 are twisted, showing that the $^{27}$Al irradiation has caused a differing phase change across the spinning sideband manifold. This is because each spinning sideband results from a different combination of crystallite orientations and dipolar couplings. Consider a simple example, where we assume that the principal axes of the quadrupolar and dipolar tensors are collinear, and consider only the extremities of the spinning sideband manifold. These spinning sidebands arise primarily from coupling to $m = \pm{}^5/_2$ $^{27}$Al states, where the dipolar coupling tensor is aligned close to (or along) the static magnetic field, after the initial $\pi/2$ excitation pulse, and at the echo. $Q$ is originally positive, thus the spins in the $m = {}^5/_2$ and $-{}^5/_2$ states will be transferred to the ${}^3/_2$ and $-{}^1/_2$ states, respectively (at different times in the rotor period). Since the $m = {}^5/_2$ and $-{}^5/_2$ states contribute to opposite sides of the sideband manifold unequal dephasing will occur, hence the phase twist.

Figure 11 shows the $\delta$ dependence of the TRAPDOR fraction, $\Delta S/S_0 = (S_0 - |S|)/S_0$, calculated with the numerical integration procedure outlined above. Note that the theory does not make predictions around zero offset. The input parameters for the calculation are indicated in the figure caption. They include the experimental parameters $\nu_R$ and $\nu_1$, the quadrupolar parameters $\nu_Q = ({}^3/_{20})e^2qQ/h$ and $\eta$, and the geometric parameters of the internuclear Al−H distance $r$ and its polar angles with respect to the EFG principal axes. The calculation produces a profile in $^{27}$Al frequency space having the same overall width as the first-order quadrupole spectrum (from $-2\nu_Q = -4$ MHz to $2\nu_Q = 4$ MHz). The figure shows that in addition to an obvious dependence of the size of the effect on $\nu_R$, $\nu_1$, and $r$, the TRAPDOR profiles are also quite sensitive to the asymmetry parameter and to the orientation of the internuclear vector with respect to the EFG tensor axes. Hence, TRAPDOR results potentially contain detailed geometric information.

Unfortunately, the present method of calculation is not sufficiently quantitative to ensure that such detailed geometric information can indeed be extracted from experimental data. The calculations are based on a number of approximations, the quantitative impact of which has not been fully explored at this time. To complete the discussion of the semiquantitative model, we now review some of its potential shortcomings. One of the

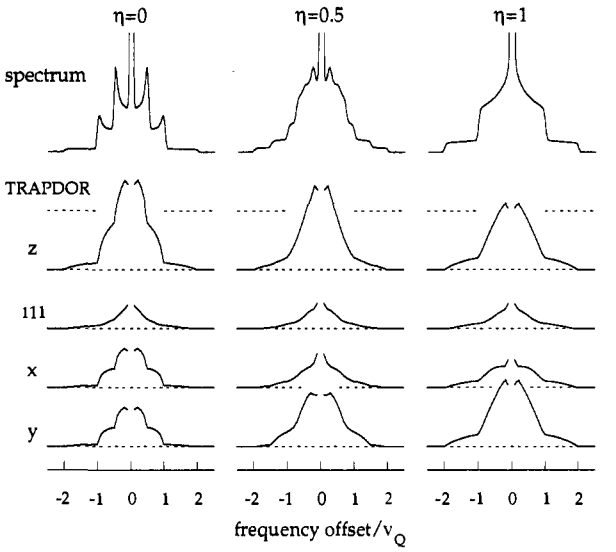


**Figure 11.** The calculated frequency-offset dependence of the TRAPDOR fraction $\Delta S/S_0$ for a proton which is dipolar coupled to an $^{27}$Al spin subject to $^{27}$Al irradiation during one rotor period. The corresponding static first-order $^{27}$Al spectra are shown in the top row (central transition truncated). The three columns were calculated for the three indicated values of $\eta$. The rows correspond to different directions of the Al−H vector with respect to the EFG principal axes system: three parallel to the $x$, $y$, and $z$ axes and one along the body diagonal [111]. Other parameters: rf amplitude = 40 kHz, sample spinning rate = 3 kHz, $\nu_Q = 2$ MHz (QCC = 13.3 MHz, $\alpha' = 0.27$), Al−H distance = 2.45 Å. The horizontal dotted lines are separated by $\Delta S/S_0$ increments of 0.5.

assumptions is that the transfers are instantaneous. In reality, a finite amount of time is spent on traversing the full width of an avoided level crossing. One may estimate from the plot in Figure 2b that the difference between the values of $Q$ on the two sides of a crossing is about $5\omega_1$ for $\pm{}^1/_2 \leftrightarrow \pm{}^3/_2$ and $2\omega_1$ for $\pm{}^3/_2 \leftrightarrow \pm{}^5/_2$. When $\nu_Q$ is 2 MHz and $\nu_1$ is 40 kHz, the time to complete such a crossing amounts to at least 1 to 2% of the rotor period, adding up to at least 6−12% for all the crossings combined, depending on the number of zero crossings of $Q$ and on the size of $\delta$. This introduces a modest error in the calculated dipolar evolution, comparable to finite-pulse-width errors in REDOR. The situation is more serious for those crystallites which reach their maximum or minimum value of $Q$ in the vicinity of a level crossing. At such turning points of $Q$ the quadrupolar spins linger for a relatively long time in ill-defined states.

Another approximation is the use of the transfer function $T(\alpha)$ for predictions of population transfer. Since it was derived from an ideal case where the crossing began far above and ended far below the resonance condition, we implicitly assume that the eigenstates between crossings are pure $m$ states. In our application with its rapid succession of the level crossings, this may be an oversimplification which could have an appreciable effect on the results.

The model also ignores the existence of off-diagonal elements in the density matrix of $S$, although it is certain that these elements are created by level crossings with intermediate adiabaticity parameters (see above). Their immediate effect on the dipolar interaction is negligibly small because of their rapid oscillation at rates of the order of the quadrupole frequency, but when the spin system lingers for a long time in the vicinity of a crossing (which, as we saw, may happen at the turning points of $Q$) the oscillations are slow, so that the off-diagonal elements have a more pronounced effect on the $I$ spins. Another complication is that the off-diagonal elements created during

one transfer are partially transferred back to the diagonal at a subsequent level crossing. Numerical integration of the full density matrix equation of a single rotating spin system has shown that this is indeed a real effect. Nonetheless, we feel justified in ignoring these off-diagonal elements because the signs of the resulting diagonal elements depend on the phases of the off-diagonal elements at the time of the second crossing such that phase randomization of the rapidly oscillating off-diagonal elements will presumably average their net impact to zero. But this does not take into account the phase correlations which may exist between successive level crossings and which could lead to some form of "refocusing" of level populations of $S$. To obtain experimental assurance that this refocusing is irrelevant to the TRAPDOR reduction of the $I$-spin signals, we modified the TRAPDOR experiment by changing the phase of the $^{27}$Al irradiation from $x$ to $-x$ and/or $\pm y$ several times during one $\tau$ period. The objective was to check whether the relative phases of the rf and the oscillating off-diagonal elements would influence the manner in which diagonal elements are resurrected. None of these experimental modifications had any effect on the TRAPDOR echo, suggesting that the refocusing of populations in the off-diagonal elements may, indeed, be ignored. Nevertheless, we are not certain that all aspects of the spin dynamics of $S$ are sufficiently understood.

Numerical calculations for $I = 1$ passages have shown that in the small $\alpha'$ regime the creation of non-spin-locked (off-diagonal) components of the density matrix becomes more important than creation of spin-locked coherences. The differences between the calculated and experimental results in the case of small $\alpha'$ (Figure 8) indicate that the inaccuracies of the theory have, indeed, practical implications in this regime: the experimentally observed TRAPDOR fraction is larger than predicted. Our theory does not take into account the additional dephasing caused by transfer of populations into mixed states, which is most likely the cause of the larger TRAPDOR fractions.

Our model does not take into account other spin interactions, such as the homonuclear proton−proton coupling. The homonuclear coupling does not commute with the chemical-shift and the heteronuclear-dipole terms in the Hamiltonian and thus invalidates the simple description of phase accumulation of the proton FID's. In a related experiment it was found that the population transfer of protons in adamantane under fast-passage conditions ($\alpha < 0.3$) appeared to have more adiabatic character than the theoretical $T(\alpha)$ dependence, as plotted in Figure 10, predicted.[12] This was ascribed to a partial transfer from Zeeman order to dipolar order due to homonuclear dipole interactions.

Finally, our theory is invalid for on-resonance irradiation. Experimentally, the largest values of $\Delta S/S_0$ are observed for irradiation at the Larmor frequency. Simple theoretical arguments based on inspection of Figure 2a are not consistent with this observation. For small resonance offsets, an adiabatic passage leaves the $^3/_2$ and $-^3/_2$ states unaffected. Hence, under conditions of adiabatic passages, at most two-thirds of the protons (i.e. only those that are coupled to $^{27}$Al spins in $\pm^1/_2$ or $\pm^5/_2$ states) are affected, limiting the TRAPDOR fraction to 67%. Since, in general, the TRAPDOR fractions decrease when the adibaticity parameter is lowered, this implies that the on-resonance value should always be well below 67%. (An indication of the onset of this effect is seen in the drop of some of the calculated TRAPDOR curves in Figures 8 and 11 at $\pm 0.5$ MHz offset.) The observed on-resonance $\Delta S/S_0$ values are, however, as large as 89%. Apparently, the simple theoretical reasoning is flawed because it underestimates the degree of mixing of *all* of the states when the passages are faster than adiabatic. This mixing will alter the dephasing of the coupled spins, leading to a TRAPDOR effect. A similar effect was also seen in the calculations for off-resonance irradiation for non-adiabatic passages, where a larger than predicted TRAPDOR fraction was also observed. Here too, the larger TRAPDOR effects were ascribed to the formation of non-spin-locked coherences (i.e. the formation of mixed states).

Another possible cause of the deviation of the experimental TRAPDOR fraction from the theoretical upper-limit prediction at the Larmor frequency is the presence of Al−H pairs which do not belong to bridging hydroxyls. As the proton and $^{27}$Al spectra showed, there is a significant remnant of ammoniated Al sites. These have a relatively small QCC and thus contribute to the TRAPDOR effect close to resonance. However, while these extra Al's can contribute to the general increased effectiveness of TRAPDOR close to resonance, they cannot account for the fact that the experimental TRAPDOR fraction in the center of the plot does not reflect the theoretical $^2/_3$ limit, in particular because the passages of the Al's with small QCC are more adiabatic than the passages of the other Al's.

JA950711A